Discriminated Release of a Hippurate-Like Radiometal Chelate in Nontarget Tissues for Target-Selective Radioactivity Localization Using pH-Dependent Dissociation of Reduced Antibody

Yasushi Arano, Tatsuo Inoue, Takahiro Mukai, Kouji Wakisaka, Harumi Sakahara, Junji Konishi and Akira Yokoyama

Faculty of Pharmaceutical Sciences and Faculty of Medicine, Kyoto University, Kyoto, Japan

To achieve high and selective target radioactivity localization by monoclonal antibodies (Mabs) labeled with metallic radionuclides, the discriminated release of a hippurate-like radiometal chelate in nontarget tissues was performed using chemically modified Mabs. **Methods:** The disulfide bonds of a Mab against osteogenic sarcoma (OST7, IgG_1) were reduced and ^{67}Ga chelate of succinyldeferoxamine (SDF) was conjugated proximal to the Mab molecule via an ester bond with exposed thiol groups (^{67}Ga-DFO-MESS-redOST7), which would impair esterase access to the ester bond of ^{67}Ga-DFO-MESS-redOST7 due to the steric interference induced by bulky antibody molecule, stabilizing the ester bond in plasma and on the target cell's surface. Gallium-67-SDF was also conjugated to OST7 via an ester bond with 2-iminothiolane to render the ester bond in a position distal from the OST7 molecule (^{67}Ga-DFO-MESS-IT-OST7). **Results:** Although SDS-PAGE analyses of ^{67}Ga-DFO-MESS-redOST7 showed a partial cleavage of its disulfide bonds, size-exclusion HPLC and cell binding assays indicated that the IgG structure and immunoreactivity of this conjugate were preserved in a neutral buffer and plasma of the systemic circulation. **Conclusion:** The present radiochemical design of an antibody utilizing pH-dependent dissociation would constitute a promising approach in establishing selective target radioactivity localization by Mabs.

Key Words: gallium-67; monoclonal antibodies; target selection

J Nucl Med 1994; 35:326–333

In radioimmunoimaging and radioimmunotherapy of tumors using monoclonal antibodies (Mabs) labeled with metallic radionuclides, the decrease in radioactivity observed in nontarget tissues such as the liver has been a subject of great importance. Various mechanisms have been reported for the radioactivity localization of Mabs labeled with metallic radionuclides in nontarget tissues. These include transchelation of the radiolabel in vivo, the presence of circulating antigens, hepatic recognition of the antibody molecule through Fc or asialo-receptors and electrostatic interaction between positively charged Mabs and negatively charged cell surfaces (*1–5*).

Recent studies on the metabolism of ^{111}In-labeled antibodies have shown that the catabolism of radiolabeled antibodies in the liver is very rapid and a slow elimination rate of radiolabeled metabolites from the liver is responsible for the prolonged radioactivity localization of ^{111}In-labeled antibodies in this organ (*5–7*). If a radiolabeled metabolite with similar biological characteristics to those of hippuric acid were to be released from antibodies during catabolism in nontarget tissues, then the radioactivity would be eliminated from these tissues.

To examine the validity of this approach, we have developed a new bifunctional reagent (MESS: N-[[4-(maleimidoethoxy)succinyl]oxy]succinimide) for the conjugation of a Mab with a hippurate-like radiometal chelate, such as the ^{67}Ga chelate of succinyldeferoxamine (SDF), via an ester bond (*8*). This ^{67}Ga-labeled Mab achieves lower radioactivity levels in nontarget tissues and manifests a higher target-to-nontarget radioactivity ratio in the athymic mice model compared with the ^{67}Ga-labeled Mab without an ester bond to release ^{67}Ga-SDF (*9,10*). This ^{67}Ga-labeled Mab, however, registered about a 20% decrease of the net radioactivity accumulated in the tumor from 24 to 48 hr postinjection. This is due to a cleavage of the ester bond and the release of ^{67}Ga-SDF not only in nontarget tissues but in plasma and tumor cell surface as well (*10*). These findings indicate that the development of radiolabeled Mabs rendering selective cleavage of the ester bond in nontarget tissues would lead to more useful radiopharmaceuticals for clinical use.

Received Jun. 15, 1993; revision accepted Oct. 20, 1993.

For correspondence and reprints contact: Akira Yokoyama, PhD, Dept. of Radiopharmaceutical Chemistry, Faculty of Pharmaceutical Sciences, Kyoto University, Sakyo-ku, Kyoto 606 Japan.

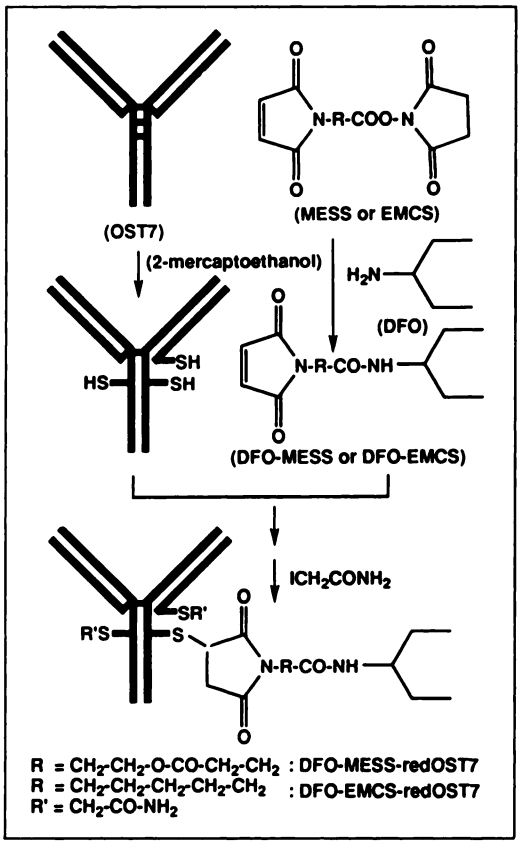

FIGURE 1. Reaction sequence for the preparation of DFO-MESS-redOST7 and DFO-EMCS-redOST7 conjugates by reducing the disulfide bonds of OST7 molecule.

Since our previous study has indicated that the effect of esterase is more important in ^{67}Ga-SDF release from conjugate than the medium pH (*8*), conjugation of ^{67}Ga-SDF at a position proximal to a Mab molecule via an ester bond would impair esterase access to the ester bond due to the steric interference induced by bulky antibody molecules. Accordingly, the reduction of the disulfide bonds of a Mab was conducted to introduce ^{67}Ga-SDF via an ester bond by utilizing the exposed thiol groups (Fig. 1). Reduction of the disulfide bonds of human nonspecific IgG and subsequent alkylation of the thiol groups has been known to preserve the original IgG structure and immunoreactivity when kept at a neutral pH environment (*11–13*). Reducing the disulfide bonds of IgG is also a biochemical approach known to prepare heavy chains, light chains and half molecules of IgG utilizing the dissociation of noncovalently bonded chains under acidic conditions (*14,15*). This dissociation characteristic of reduced antibodies at a lower pH would facilitate cleavage of the ester bond and induce release of ^{67}Ga-SDF, accompanied by nullification of the steric interference of the antibody molecule due to chain dissociation and proteolysis in lower pH environment of nontarget tissues. In this study, the biological properties and in vivo metabolic fate of ^{67}Ga-labeled OST7s (Figs. 1 and 2) were investigated to evaluate if the present radiochemical Mab design could improve the efficiency of tumor-selective radioactivity localization in normal and athymic mice.

MATERIALS AND METHODS

All chemicals were of reagent grade and were used without further purification. MESS was synthesized as described previously (*8*). SDF was synthesized according to the procedure of Herscheid et al. (*16*). N-(E-maleimidocaproyloxy)succinimide (EMCS) was purchased from Dojindo Laboratories (Kumamoto, Japan).

Tumor and Monoclonal Antibody

KT005-cloned human osteogenic sarcoma was maintained by serial subcutaneous transplantation in athymic mice. One to 2 mm^3 tumor tissues (0.5–1.0 g) at 2 to 3 wk postplantation were used for the in vivo study. Single cell suspensions from xenografted tumors (*17,18*) were used for the in vitro study.

The Mab against osteogenic sarcoma (OST7, IgG_1), generated by standard hybridoma technology, was purified by sodium sulfate precipitation with follow-up protein-A affinity column chromatography (Pharmacia Biotech Co. Ltd., Tokyo, Japan) (*17,18*).

Preparation of DFO-MESS-redOST7 and DFO-EMCS-redOST7

DFO-MESS-redOST7 was prepared by reducing the disulfide bonds of OST7 (*19*) with the following modifications (Fig. 1): OST7 was concentrated in a nitrogen atmosphere to 10 mg/ml in well-degassed 0.1 *M* phosphate buffered-saline (PBS, pH 7.0) containing 2 m*M* of ethylenediaminetetraacetic acid (EDTA) using the Diaflow system (8 MC model, Amicon Grace, Tokyo, Japan). The antibody was allowed to react with 4.55 μl of 2-mercaptoethanol (2-ME, 1000 molar excess) by gently stirring at room temperature for 30 min. Excess 2-ME was then removed by the

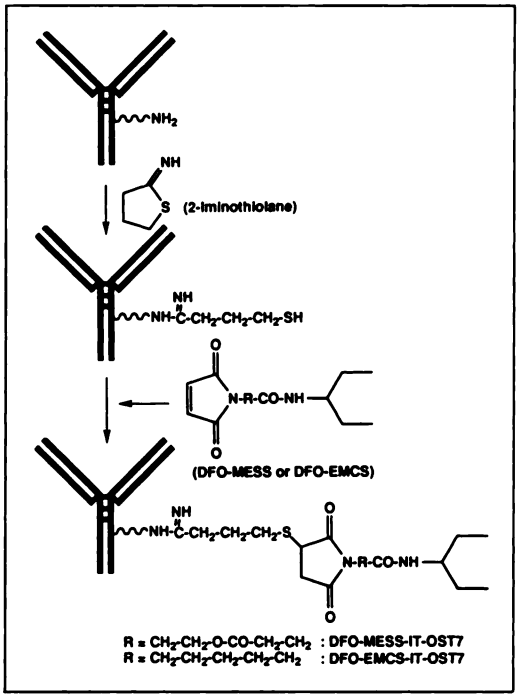

FIGURE 2. Reaction sequence for the preparation of DFO-MESS-IT-OST7 and DFO-EMCS-IT-OST7 conjugates utilizing 2-iminothiolane. DFO-MESS and DFO-EMCS were prepared according to the procedures as shown in Figure 1.

Diaflow system (8 MC) with 20 volumes of well-degassed 0.1 *M* PBS containing 2 m*M* EDTA (pH 6.0) before adjusting the protein concentration to 5 mg/ml. A small portion of this mixture was sampled, and the number of exposed thiol groups was estimated with 2,2'-dithiodipyridine (*20*). MESS (40 m*M*) in dimethylformamide (100 μl) was added to an equal volume of 80 m*M* deferoxamine (DFO) in 0.05 *M* borate-buffered saline (pH 8.2). The reaction mixture was then stirred for 30 min at room temperature prior to adding 200 μl of this solution to a freshly thiolated OST7 solution. After agitating the reaction mixture gently for 2 hr at room temperature, 7.4 mg of iodoacetamide was added. The mixture was stirred for an additional 30 min to alkylate the nonreacted thiol groups. The DFO-MESS-redOST7 conjugate was separated from the nonreacted small molecules using Sephacryl S-200 column chromatography (1.8 × 40 cm) equilibrated and eluted with 0.1 *M* PBS (pH 6.0). The conjugate fractions were finally collected and concentrated to 1 mg/ml by ultrafiltration (8 MC). DFO-EMCS-redOST7 was also synthesized according to the procedure described above except EMCS was used in place of MESS (DFO-EMCS-redOST7).

Preparation of DFO-MESS-IT-OST7 and DFO-EMCS-IT-OST7

Forty-five microliters of 2-iminothiolane (2-IT, 1 mg/ml) prepared in the same buffer was added to 1 ml of well-degassed OST7 solution (10 mg/ml) in 0.16 *M* borate buffer (pH 8.0) containing 2 m*M* EDTA. The reaction mixture was gently stirred at room temperature for 1 hr. Nonreacted reagent was removed by the Diaflow system (8 MC) with 20 volumes of well-degassed 0.1 *M* PBS containing 2 m*M* EDTA (pH 6.0), and the protein concentration was adjusted to 5 mg/ml. The reaction solution (120 μl) of MESS and DFO, prepared according to the procedure described above, was added to the freshly thiolated OST7 solution. The reaction mixture was stirred at room temperature for 2 hr. The conjugate was purified by Sephacryl S-200 column chromatography and eluted with 0.1 *M* PBS (pH 6.0) before adjusting to 1 mg/ml (DFO-MESS-IT-OST7). In a similar manner, DFO-EMCS-IT-OST7 was prepared according to the procedure described above except EMCS was used instead of MESS (Fig. 2). Each conjugate was characterized by SDS-PAGE (Mini PROTEAN II, Bio-rad Co. Ltd., Richmond, CA) under both reducing and nonreducing conditions using 4%–20% gradient gels (Bio-rad Co. Ltd.).

Conjugate Radiolabeling

Varying amounts of ^{67}Ga-citrate (50–400 μl, 1 mCi/ml) were added to 1 ml solution of each conjugate (1 mg/ml) before the reaction mixtures were incubated at room temperature for 2 hr. The labeling efficiency was determined by size-exclusion HPLC (5Diol-300, 7.5 mm × 60 cm, Nacalai Tesque, Kyoto, Japan) eluted with 0.1 *M* PBS (pH 6.8) at a flow rate of 1 ml/min, paper chromatography (No. 50, Advantec Toyo Ltd., Tokyo, Japan) developed with saline, and celluloseacetate electrophoresis run at an electrostatic field of 0.8 mA/cm for 45 min.

OST7 was also labeled with ^{125}I by the chloramine T method (*18*). Radiolabeling of DFO and SDF was carried out using saline solution (1 mg/ml) of each ligand with 50–100 μl ^{67}Ga-citrate.

Immunoreactivity Measurement

The immunoreactivity of each ^{67}Ga-labeled OST7 was determined according to the procedure as described before (*17,18*). Tumor cells (2×10^4–5×10^6) suspended in 100 μl of Dulbecco's PBS were incubated with 100 μl of radiolabeled OST7 in a microcentrifugation tube (5.7 × 46 mm) for 2 hr at 4°C. After centrifugation at 10,000 × g for 5 min, the supernatant was discarded and the radioactivity was determined (Beckman Co. Ltd., Gamma 5500, Tokyo, Japan).

Plasma Stability of the Ester Bond

Gallium-67-labeled OST7 (20 μl) was added to a mixture of 115 μl of freshly prepared murine plasma and 115 μl of 20 m*M* tris-HCl buffer (pH 7.5). The reaction mixture was incubated for 24 hr at 37°C prior to analyses of each sample by celluloseacetate electrophoresis under the same conditions as described above.

In Vivo Study

Each ^{67}Ga-labeled OST7 was diluted with 0.1 *M* PBS (pH 6.0) and the antibody concentration was adjusted to 0.4 mg/ml. Biodistribution studies of each ^{67}Ga-labeled OST7 were performed in 6-wk-old male ddY mice at 1, 3, 6, 24 and 48 hr after intravenous injection (*21*). Groups of five mice, each received 20 μg of the respective ^{67}Ga-labeled OST7, were used for the experiments. Organs of interest were isolated, weighed and the radioactivity was counted. Athymic mice bearing osteogenic sarcoma were treated intravenously with ^{67}Ga-DFO-MESS-redOST7, ^{67}Ga-DFO-MESS-IT-OST7 and ^{67}Ga-DFO-EMCS-IT-OST7 (20 μg each) prior to killing the animals at 24 and 48 hr postadministration. Organs of interest were similarly isolated, and the radioactivity was determined.

To investigate the metabolism of ^{67}Ga-DFO-MESS-redOST7 in the liver and kidney, doses of 20 μg were intravenously injected in 6-wk-old ddY mice. At 24 hr postinjection, the mice were treated according to the procedure of Motta-Hennessy et al. under ether anesthesia (*7*) with slight modifications (*10*). The liver and kidneys were perfused in situ with 2 ml cold 0.1 *M* tris-citrate buffer (pH 6.5) containing 0.15 *M* NaCl, 0.002% sodium azide, 1 TIU/ml aprotinin, 2 m*M* benzamide-HCl, 2 m*M* iodoacetamide and 5 m*M* diisopropyl fluorophosphate. One gram each of the organs was excised, placed in a plastic tube and subjected to three cycles of freezing (dry ice-acetone bath) and thawing. Five ml of the buffer containing an additional 35 m*M* of beta-octyl-glucoside was then added to each tube. The liver and kidneys were homogenized by cell disruption with a polytron homogenizer (PT 10-35, Kinematica GmbH, Littau, Switzerland) at full speed for three 30-sec bursts, followed by centrifugation at 48,000x g for 20 min (Himac CS-120 centrifuge; Hitachi Co Ltd., Tokyo, Japan). Supernatants were separated from the pellets and the radioactivity was counted. Following filtration through a polycarbonate membrane with a pore diameter of 0.22 μm (Myrex, Millipore Ltd., Tokyo, Japan), the supernatants were analyzed by the size-exclusion HPLC under identical analytical conditions as described above. Fractions (1 ml) were subsequently collected and the radioactivity counts determined.

At 24 and 48 hr postinjection of ^{67}Ga-DFO-MESS-redOST7 or ^{67}Ga-DFO-EMCS-redOST7 (150 μl, 100 μg) in 6-wk-old ddY mice, blood samples of mice killed under ether anesthesia were collected. After centrifugation at 1,500x g, plasma was isolated, filtered through a polycarbonate membrane (0.22 μm) before analysis by size-exclusion HPLC was performed under the conditions described above.

At 24 hr postinjection of ^{67}Ga-DFO-MESS-redOST7 (300 μl, 200 μg) in 6-wk-old ddY mice, urine samples were collected and filtered through a 10,000 Da cut-off ultrafiltration membrane (Millipore Ltd., Tokyo, Japan) before analysis by reverse-phase HPLC (Cosmosil $5C_{18}$-AR, 4.6 × 250 mm, Nacalai Tesque, Kyoto, Japan). The reverse-phase HPLC was performed using a mixture of methanol and 10 m*M* aqueous ammonium acetate (1:1)

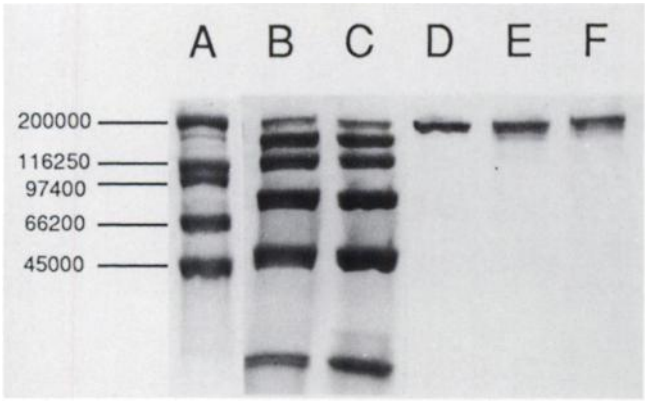

FIGURE 3. SDS-PAGE profiles of the four conjugates under nonreducing conditions. Molecular weight standards (in column A) are myosin (200000 Da), beta-galactosidase (116250 Da), phosphorylase b (97400 Da), bovine serum albumin (66200 Da) and ovalbumin (45000 Da). While 2-iminothiolane-modified DFO-MESS-IT-OST7 (E) and DFO-EMCS-IT-OST7 (F) each indicated a single band corresponding to the unmodified OST7 (D), both DFO-MESS-redOST7 (B) and DFO-EMCS-redOST7 (C) demonstrated six bands corresponding to H_2L_2 (intact IgG), H_2L, H_2, HL, H (heavy chain) and L (light chain), respectively. Partial cleavages of interchain disulfide bonds of the latter two conjugates were thus demonstrated.

as an eluent at a flow rate of 1 ml/min. HPLC analyses of the urine sample were also carried out in the presence of either ^{67}Ga-SDF or ^{67}Ga-DFO, accordingly.

RESULTS

In Vitro Studies

OST7 was reduced with 2-ME to expose 6 to 7 molecules of thiol groups per molecule of OST7. The 2-IT modification introduced 1 to 1.3 molecules of thiol groups per molecule of the protein. Size-exclusion HPLC analyses for each of the conjugates revealed a single UV (280 nm) peak with a retention time (13.2 min) similar to that of the unmodified OST7. SDS-PAGE analyses under reducing conditions indicated that all the conjugates showed two typical bands at 50,000 and 25,000 Da. In SDS-PAGE analyses under nonreducing conditions, DFO-MESS-IT-OST7 and DFO-EMCS-IT-OST7 conjugates indicated a single band corresponding to that of the unmodified OST7 molecule at 150,000 Da. However, DFO-MESS-redOST7 and DFO-EMCS-redOST7 conjugates exhibited six bands, ranging from 25,000 to 150,000 Da (Fig. 3).

Radiolabeling of the four conjugates with ^{67}Ga-citrate attained a radiochemical yield exceeding 93% when analyzed by paper chromatography, celluloseacetate electrophoresis and size-exclusion HPLC. Consequently, all the conjugates were used without further purification. The size-exclusion HPLC radioactivity profiles of ^{67}Ga-DFO-MESS-redOST7 and ^{67}Ga-DFO-MESS-IT-OST7 superimposed on the spectrophotometric elution profile of unmodified OST7 at 280 nm (Fig. 4). Similarly, both ^{67}Ga-DFO-EMCS-redOST7 and ^{67}Ga-DFO-EMCS-IT-OST7 overlapped on a single peak of the unmodified OST7 fraction (data not shown).

Figure 5 shows the bindings of ^{67}Ga- and ^{125}I-labeled OST7 to KT005 cells as a function of the cell number. We observed no significant difference between ^{67}Ga-labeled redOST7 (prepared by reducing the disulfide bonds) and ^{125}I-labeled OST7 (Fig. 5A). Similar results were observed between ^{67}Ga-labeled IT-OST7 (prepared by the 2-IT method) and ^{125}I-OST7 (Fig. 5B).

When each conjugate was incubated in 50% diluted plasma at 37°C for 24 hr, ^{67}Ga-DFO-MESS-redOST7 released 5.08% (±0.6%) of the radioactivity, whereas the radioactivity released from ^{67}Ga-DFO-MESS-IT-OST7 was 16.4% (±1.56%). Under similar experimental conditions, less than 5% of the radioactivity was released from both ^{67}Ga-DFO-EMCS-redOST7 and ^{67}Ga-DFO-EMCS-redOST7.

In Vivo Studies

The radioactivity distributions after intravenous administration of ^{67}Ga-DFO-MESS-IT-OST7 and ^{67}Ga-DFO-EMCS-IT-OST7 in normal mice were investigated in vivo (Fig. 6). Gallium-67-DFO-MESS-IT-OST7 showed a faster radioactivity clearance rate from the circulation and registered lower accumulations in the liver, kidneys and spleen compared with ^{67}Ga-DFO-EMCS-IT-OST7. The radioactivity distributions in normal mice after intravenous injections of ^{67}Ga-DFO-MESS-redOST7 and ^{67}Ga-DFO-EMCS-redOST7 indicated an appropriately identical radioactivity clearance from the circulation with different radioactivity localizations in the organ, respectively (Fig. 7). Although ^{67}Ga-DFO-EMCS-redOST7 manifested radioactivity accumulations in liver and kidneys, ^{67}Ga-DFO-MESS-redOST7 recorded lower values in these organs.

Figure 8 shows the size-exclusion HPLC radioactivity profiles of the liver (A) and kidney (B) extracts of mice 24 hr after injection with ^{67}Ga-DFO-MESS-redOST7. The efficiency of radioactivity extraction from the tissue homogenates was over 90%. In both extracts, all radioactivity counts were detected in the high molecular weight fractions whose retention times were similar to that of unmodified OST7. Under these analytical conditions, small molecular weight compounds, such as ^{67}Ga-SDF and ^{67}Ga-DFO, were eluted around 25 min.

Size-exclusion HPLC radioactivity profiles of murine plasma 24 and 48 hr after ^{67}Ga-DFO-EMCS-redOST7 ad-

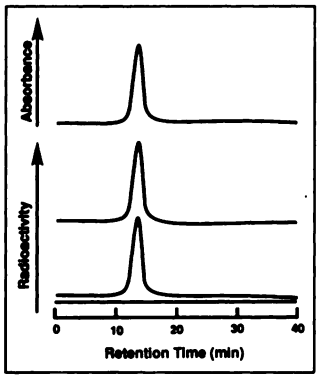

FIGURE 4. Size-exclusion HPLC profiles of unmodified OST7 (top), ^{67}Ga-DFO-MESS-IT-OST7 (middle), and ^{67}Ga-DFO-MESS-redOST7 (bottom). Both ^{67}Ga-labeled OST7 showed a single elution profile with a retention time similar to that of unmodified OST7, indicating that both ^{67}Ga-labeled OST7s existed as an intact IgG form around neutral pH. Absorbance was designated at UV 280 nm.

ministrations are shown in Figure 9A. At each postinjection time, the retention times of all radioactivity peaks were identical to that of the original ^{67}Ga-DFO-EMCS-redOST7. Similar results were obtained with the use of ^{67}Ga-DFO-MESS-redOST7 (data not shown). The reverse-phase HPLC analyses of urine samples of mice 24 hr after ^{67}Ga-DFO-MESS-redOST7 injection (Fig. 9B) indicated a single radioactivity peak at 4.4 min even when analyzed in the presence of ^{67}Ga-SDF. However, the urine sample showed two separated radioactivity peaks when analyzed in the presence of ^{67}Ga-DFO.

Comparative biodistribution of radioactivity in athymic mice bearing osteogenic sarcoma 24 and 48 hr after injections of ^{67}Ga-DFO-MESS-redOST7, ^{67}Ga-DFO-MESS-IT-OST7 and ^{67}Ga-DFO-EMCS-IT-OST7 were presented in Table 1. In tumors, ^{67}Ga-DFO-MESS-redOST7 demonstrated a radioactivity localization either higher than or comparable to those of ^{67}Ga-DFO-MESS-IT-OST7 and ^{67}Ga-DFO-IT-EMCS-OST7 between 24 and 48 hr postinjection, respectively. A decreased radioactivity localization from the tumor within the same postinjection interval was registered by ^{67}Ga-DFO-MESS-IT-OST7. In nontarget tissues, although a high radioactivity count in the liver was obtained with ^{67}Ga-DFO-EMCS-IT-OST7, the count was reduced with both ^{67}Ga-DFO-MESS-redOST7 and ^{67}Ga-DFO-MESS-IT-OST7, each possessing an ester bond to release the ^{67}Ga-SDF. When the tumor-to-organ radioactivity ratios of the three ^{67}Ga-labeled OST7s were compared (Fig. 10), ^{67}Ga-DFO-MESS-redOST7 demonstrated the highest value with no significant differences verified between ^{67}Ga-DFO-MESS-IT-OST7 and ^{67}Ga-DFO-EMCS-IT-OST7 at both postinjection times.

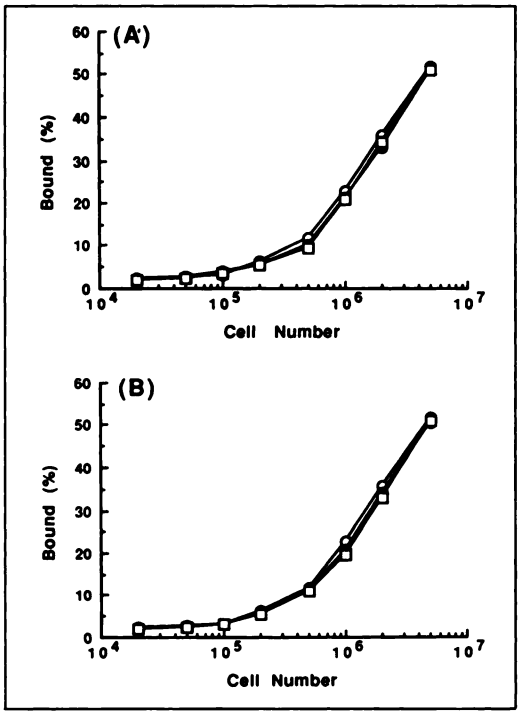

FIGURE 5. Reactivity of radiolabeled OST7s with KT005 cells. Radioactivity bound to cells (%) was plotted against the cell number. Both ^{67}Ga-DFO-MESS-redOST7 (●) and ^{67}Ga-DFO-EMCS-redOST7 (□) showed a binding activity with KT005 cells identical to that of ^{125}I-OST7 (○) (A). Similar results were observed between the two 2-IT-modified OST7 (^{67}Ga-DFO-MESS-IT-OST7 (●), ^{67}Ga-DFO-EMCS-IT-OST7 (□)) and ^{125}I-OST7 (○) (B).

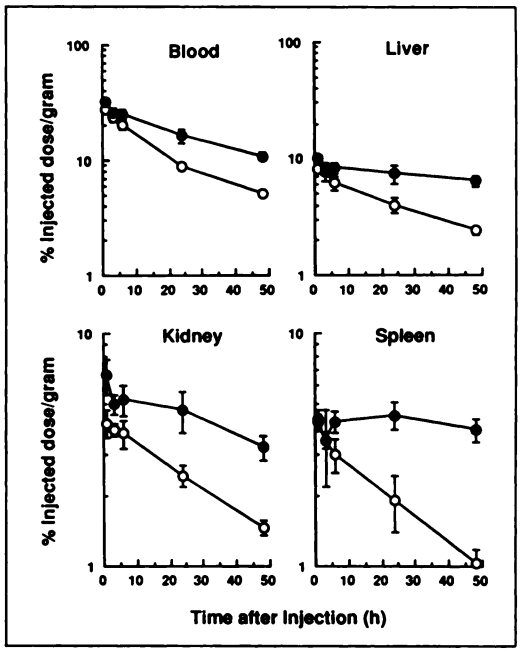

FIGURE 6. Comparative radioactivity biodistribution after intravenous injections of ^{67}Ga-DFO-MESS-IT-OST7 (○) and ^{67}Ga-DFO-EMCS-IT-OST7 (●) in normal mice. The former demonstrated a faster clearance rate of radioactivity from the circulation and organs than that of the latter.

DISCUSSION

The use of Mabs labeled with metallic radionuclides has been hindered by poor radioactivity localization in the target and high radioactivity localization in nontarget tissues such as the liver. While studies to enhance target radioactivity localization are very important (*22,23*), approaches to enhance target-to-nontarget radioactivity ratios would be complementary for further application of radiolabeled Mabs in clinical studies. As a mean to reduce radioactivity from nontarget tissues with a minimum decrease in radioactivity delivered to the target by antibodies, the discriminated release of a hippurate-like radiometal chelate, ^{67}Ga-SDF, in nontarget tissues was investigated by utilizing pH-dependent dissociation characteristics of reduced antibodies. Conjugation of ^{67}Ga-SDF at a position proximal to OST7 molecule via an ester bond was rendered possible through the use of thiol groups generated as a result of reducing disulfide bonds of OST7 (^{67}Ga-DFO-MESS-redOST7). For comparison, ^{67}Ga-SDF was conjugated to OST7 by an ester bond with 2-iminothiolane to place the ester bond to a position distal from the antibody molecule (^{67}Ga-DFO-MESS-IT-OST7). Furthermore, the two ^{67}Ga-labeled OST7s were prepared by the two thiolation meth-

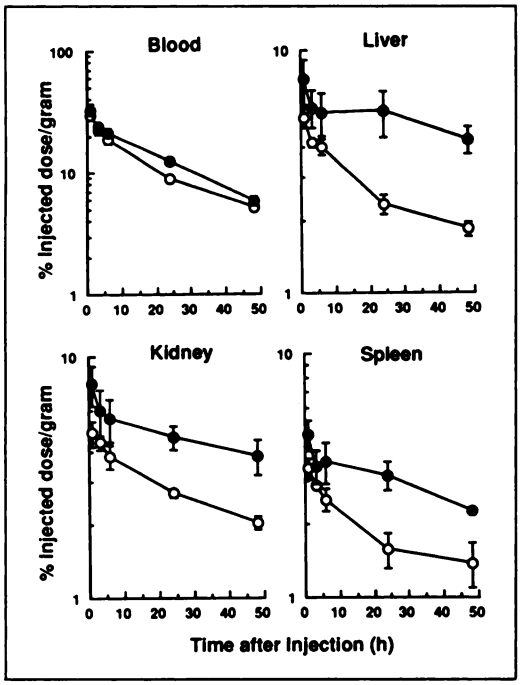

FIGURE 7. Comparative radioactivity biodistribution after intravenous administrations of ^{67}Ga-DFO-MESS-redOST7 (○) and ^{67}Ga-DFO-EMCS-redOST7 (●) in normal mice. While ^{67}Ga-DFO-MESS-redOST7 indicated a clearance rate of radioactivity from the circulation comparable to ^{67}Ga-DFO-EMCS-redOST7, ^{67}Ga-DFO-MESS-redOST7 displayed lower radioactivity localizations in the liver, kidney and spleen.

ods using EMCS (^{67}Ga-DFO-EMCS-redOST7 and ^{67}Ga-DFO-EMCS-IT-OST7), as shown in Figures 1 and 2.

Reduction of the disulfide bonds of OST7 by 2-ME liberated six to seven thiol groups for each IgG molecule. Not only did subsequent alkylation of the thiol groups with either MESS-DFO or EMCS-DFO followed by iodoacetamide not alter the size-exclusion HPLC profiles in the neutral buffer (Fig. 4) and plasma of the systemic circulation (Fig. 9A), but the original immunoreactivity (Fig. 5) as well. However, SDS-PAGE analyses of these conjugates under nonreducing conditions demonstrated six bands that corresponded well to intact IgG (H_2L_2), H_2L, H_2, HL, heavy chain (H) and light chain (L), accordingly. These indicate a partial absence of the inter-chain disulfide bonds of the OST7 molecule (Fig. 3), suggesting that ^{67}Ga-labeled redOST7 assumed an H_2L_2 form at neutral pH. This is supported by previous findings of the H_2L_2 form of reduced rabbit IgG at neutral pH values (*11,12*).

In biodistribution studies of normal mice, different radioactivity distributions among the four ^{67}Ga-labeled OST7s were observed. Of the two 2-IT-modified OST7s, ^{67}Ga-DFO-MESS-IT-OST7 showed a much faster systemic radioactivity clearance than ^{67}Ga-DFO-EMCS-IT-OST7 (Fig. 6). As was shown in the in vitro plasma incubation study, ^{67}Ga-DFO-MESS-IT-OST7 released the highest radioactivity count of the four ^{67}Ga-labeled OST7s. The above results summarize that ^{67}Ga-SDF is released from ^{67}Ga-DFO-MESS-IT-OST7 in various tissues. The most noted difference in radioactivity distribution was observed between the two ^{67}Ga-labeled OST7s, which were prepared by reducing the disulfide bonds. In spite of a similar radioactivity clearance displayed by the two ^{67}Ga-labeled redOST7s from circulation, ^{67}Ga-DFO-MESS-redOST7 demonstrated much lower radioactivity localizations in the liver and kidneys than ^{67}Ga-DFO-EMCS-redOST7 (Fig. 7). These results along with the findings of in vitro plasma incubation studies strongly imply that the ester bond of ^{67}Ga-DFO-MESS-redOST7, although stable in plasma, would be cleaved in nontarget tissues such as the liver and kidney. This discriminated cleavage of the ester bond was supported by findings of HPLC analyses of the liver and kidney supernatants. The ^{67}Ga radioactivity was present in fractions of the liver and kidneys only with a high molecular weight, indicating that the radiolabeled metabolites of small molecular weights were excreted from these tissues (Fig. 8). Although similar results were observed in the liver homogenates of mice receiving radioiodinated antibodies, high as well as low molecular weight radioactive fractions were detected in the liver homogenates after injection of ^{111}In-DTPA-labeled antibodies (*6*). Furthermore, the reverse-phase HPLC analyses of the urine samples suggested that the radioactivity was excreted from these tissues into urine as ^{67}Ga-SDF (Fig. 9B).

The ability of ^{67}Ga-DFO-MESS-redOST7 to portray a discriminated cleavage of the ester bond with a subsequent release of ^{67}Ga-SDF in nontarget tissues was well reflected

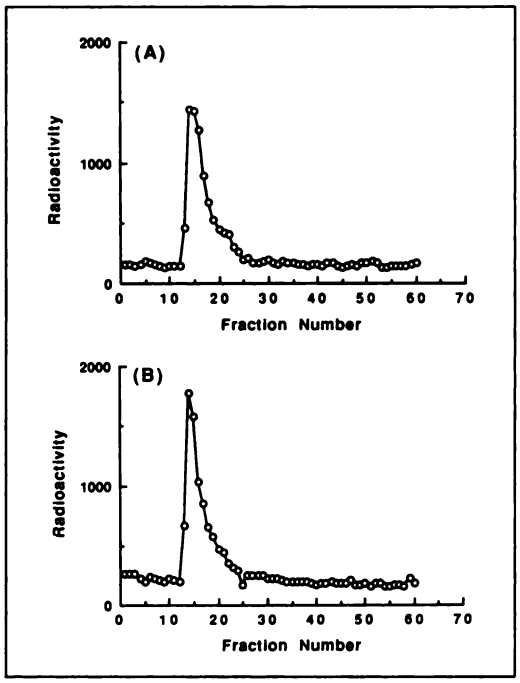

FIGURE 8. Size-exclusion HPLC analyses of the radioactivity accumulated in the liver (A) and kidney (B) supernatants 24 hr after intravenous injection of ^{67}Ga-DFO-MESS-redOST7 in normal mice. Fractions were collected at 1-min intervals. In both cases, all the radioactivity was eluted in the high molecular weight fraction with most of it present in the ^{67}Ga-DFO-MESS-redOST7 fraction.

in the biodistribution studies in athymic mice (Table 1). This radiolabeled OST7 indicated radioactivity localization levels that were comparable to and higher than those of ^{67}Ga-DFO-EMCS-IT-OST7 and ^{67}Ga-DFO-MESS-IT-OST7 in the tumor, respectively. At the same time, ^{67}Ga-DFO-MESS-redOST7 demonstrated radioactivity localization levels that were comparable to and lower than those of ^{67}Ga-DFO-MESS-IT-OST7 and ^{67}Ga-DFO-EMCS-IT-OST7 in the liver and kidneys, respectively. This was more clearly demonstrated in the tumor-to-organ ratios (Fig. 10). Gallium-67-DFO-MESS-redOST7 demonstrated the highest radioactivity ratios at both postinjection times. Insignificant differences between ^{67}Ga-DFO-MESS-IT-OST7 and ^{67}Ga-DFO-EMCS-IT-OST7 were probably due to the time-dependent radioactivity decrease of ^{67}Ga-DFO-MESS-IT-OST7 from not only the nontarget tissues but also the tumors. Thus, ^{67}Ga-DFO-MESS-redOST7 compensated the disadvantage of ^{67}Ga-DFO-MESS-IT-OST7 in bond cleavage while preserving its excretory ability of the radioactivity accumulated in the nontarget tissues. This discriminated cleavage of the ester bond might have been due to steric interference of the OST7 molecule, which could have portrayed as an intact H_2L_2 structure (Figs. 4 and 9A). This hindered esterase access to the ester bond in the plasma and on the tumor cell surface. However, radioactivity in nontarget tissues was eliminated by cleavage of the ester bond and release of ^{67}Ga-SDF, following the disappearance of steric effects of the OST7 molecule due to dissociation and proteolysis of ^{67}Ga-DFO-MESS-redOST7 into smaller fragments in lower pH environment (endosome or lysosome).

In conclusion, reduction of the disulfide bonds of Mabs and the subsequent introduction of a hippurate-like ^{67}Ga-SDF chelate via an ester bond preserved the ability of the Mab to deliver radioactivity to tumor tissues while facilitating the release of ^{67}Ga-SDF chelate in nontarget tissues. As a result, the high and selective radioactivity delivery was achieved. This radiochemical design of Mabs, utilizing the pH-dependent dissociation of the noncovalently bonded chains of the reduced and alkylated IgG accompanied by the release of hippurate-like radiometal chelates, would provide a good base to enhance target selective radioactivity localization in future studies. Mabs labeled with a variety of radionuclides such as ^{111}In, ^{186}Re, ^{188}Re and ^{90}Y may therefore be potential candidates for future clinical applications.

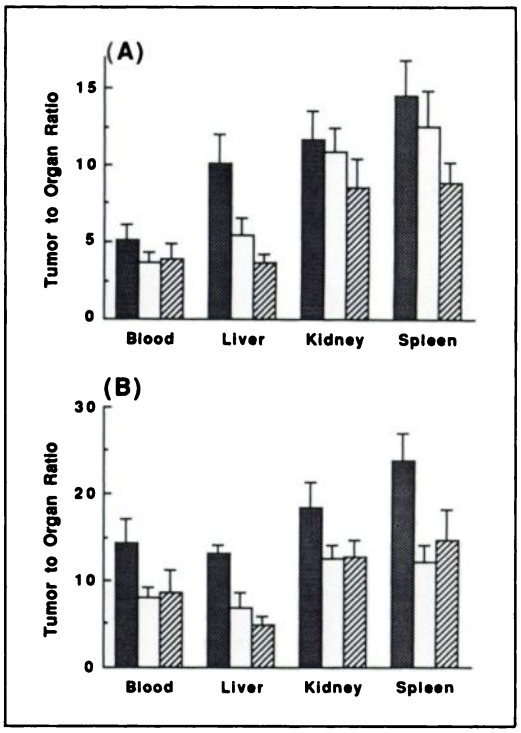

FIGURE 10. Tumor-to-organ radioactivity ratios at 24 hr (A) and 48 hr (B) after intravenous injections of ^{67}Ga-DFO-MESS-redOST7 ( ), ^{67}Ga-DFO-MESS-IT-OST7 ( ) and ^{67}Ga-DFO-EMCS-IT-OST7 ( ) in athymic mice bearing osteogenic sarcoma. Although ^{67}Ga-DFO-MESS-redOST7 and ^{67}Ga-DFO-MESS-IT-OST7 indicated radioactivity levels in nontarget tissues lower than those of ^{67}Ga-DFO-EMCS-IT-OST7 (Table 1), no significant differences were observed between the latter two ^{67}Ga-labeled OST7s in tumor-to-organ ratios. However, ^{67}Ga-DFO-MESS-redOST7 showed the highest tumor-to-organ ratios at both postinjection times. These results demonstrated that ^{67}Ga-DFO-MESS-redOST7 displayed selective radioactivity localization in targeted tumors.

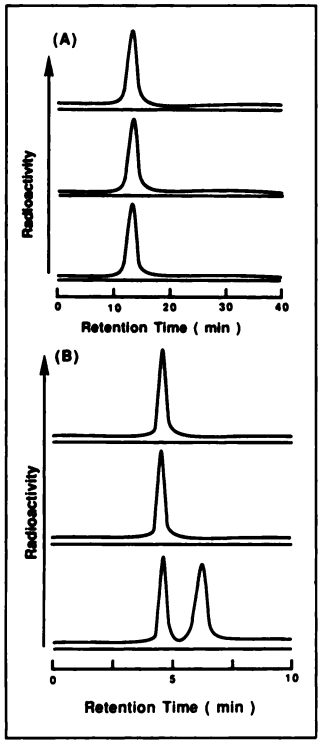

FIGURE 9. (A) Size-exclusion HPLC profiles of the radioactivity in plasma 24 (top) and 48 hr (middle) after intravenous injection of ^{67}Ga-DFO-EMCS-redOST7. The HPLC profile of ^{67}Ga-DFO-EMCS-redOST7 before injection (bottom). At both postinjection times, radioactivity was detected in the original fraction. (B) Reverse-phase HPLC analyses of urine samples obtained from mice at 24 hr postinjection of ^{67}Ga-DFO-MESS-redOST7 (top), cochromatographed with ^{67}Ga-SDF (middle) and ^{67}Ga-DFO (bottom). The urine samples showed a single radioactivity peak at a retention time similar to that of ^{67}Ga-SDF, even in the cochromatography with ^{67}Ga-SDF.

ACKNOWLEDGMENTS

The authors thank Daiichi Radioisotope Labs, Ltd., Tokyo, Japan, for providing ^{67}Ga-citrate. This work was supported in part by a Grant-in-Aid for Developing Scientific Research (# 02151072) from the Ministry of Education, Science and Culture of Japan.

TABLE 1
Radioactivity Biodistributions After Intravenous Injections of ^{67}Ga-DFO-MESS-redOST7, ^{67}Ga-DFO-MESS-IT-OST7 and ^{67}Ga-DFO-EMCS-IT-OST7 in Athymic Mice Bearing Osteogenic Sarcoma

	^{67}Ga-DFO-MESS-redOST7		^{67}Ga-DFO-MESS-IT-OST7		^{67}Ga-DFO-EMCS-IT-OST7	
Tissue*	24 hr	48 hr	24 hr	48 hr	24 hr	48 hr
Tumor	31.44 (3.33)	29.68 (3.32)	22.63 (4.55)	16.22 (5.75)	28.76 (3.56)	30.30 (3.48)
Blood	6.49 (1.06)	2.50 (1.43)	5.59 (1.94)	2.04 (0.66)	6.92 (1.44)	4.22 (1.28)
Liver	3.11 (0.52)	2.18 (0.45)	3.91 (1.16)	1.68 (0.24)	9.44 (2.90)	6.20 (1.45)
Kidney	2.69 (0.54)	1.89 (0.14)	2.00 (0.51)	0.98 (0.19)	3.42 (0.46)	2.21 (0.36)
Spleen	2.12 (0.75)	1.29 (0.36)	1.71 (0.51)	0.94 (0.17)	3.25 (0.56)	2.14 (0.58)
Intestine	1.45 (0.49)	0.79 (0.29)	0.98 (0.43)	0.56 (0.14)	1.83 (0.29)	1.00 (0.23)
Lung	3.05 (0.43)	1.44 (0.58)	2.35 (0.56)	0.98 (0.37)	3.62 (0.87)	2.23 (0.77)
Muscle	0.76 (0.17)	0.64 (0.37)	0.53 (0.11)	0.30 (0.14)	0.89 (0.25)	0.57 (0.20)

*Expressed as percent injected dose per gram wet weight as the mean (1 s.d.) for five animals each point.

REFERENCES

1. Esteban JM, Schlom J, Gansow OA, et al. New method for the chelation of indium-111 to monoclonal antibodies: biodistribution and imaging of athymic mice bearing human colon carcinoma xenografts. *J Nucl Med* 1987;28: 861–870.
2. Beatty BG, Beatty JD, Williams LE, Paxton RJ, Shively JE, O'Connor-Tressel M. Effect of specific antibody pretreatment on liver uptake of ^{111}In-labeled anticarcinoembryonic antigen monoclonal antibody in nude mice bearing human colon cancer xenografts. *Cancer Res* 1989;49:1587–1594.
3. Adams GP, DeNardo SJ, Deshpande SV, et al. Effect of mass of ^{111}In-benzyl-EDTA monoclonal antibody on hepatic uptake and processing in mice. *Cancer Res* 1989;49:1707–1711.
4. Khaw BA, Klibanov A, O'Donnell SM, et al. Gamma imaging with negatively charge-modified monoclonal antibody: modification with synthetic polymers. *J Nucl Med* 1991;32:1742–1751.
5. Paik CH, Sood VK, Le N, et al. Radiolabeled products in rat liver and serum after administration of antibody-amide-DTPA-indium-111. *Nucl Med Biol* 1992;19:517–522.
6. Himmelsbach M, Wahl RL. Studies on the metabolic fate of ^{111}In-labeled antibodies. *Nucl Med Biol* 1989;16:839–845.
7. Motta-Hennessy C, Sharkey RM, Goldenberg DM. Metabolism of indium-111-labeled murine monoclonal antibody in tumor and normal tissue of the athymic mouse. *J Nucl Med* 1990;31:1510–1519.
8. Arano Y, Matsushima H, Tagawa M, et al. A novel bifunctional metabolizable linker for the conjugation of antibodies with radionuclides. *Bioconj Chem* 1991;2:71–76.
9. Arano Y, Matsushima H, Tagawa M, et al. Search for radiolabeled antibodies with high target-to-nontarget ratio. *J Lab Compds Radiopharm* 1991; 30:312–313.
10. Arano Y, Matsushima H, Tagawa M, et al. A newly designed radioimmunoconjugate releasing a hippurate-like radiometal chelate for enhanced target-to-nontarget radioactivity. *Nucl Med Biol* 1994;21: in press.
11. Dorrington KJ, Tanford C. Molecular size and conformation of immunoglobulins. *Adv Immunol* 1972;12:333–381.
12. Painter RG, Sage HJ, Tanford C. Contribution of heavy and light chains of rabbit immunoglobulin G to activity. II. Activities of reconstituted immunoglobulin. *Biochemistry* 1972;11:1338–1345.
13. Schroeder DD, Tankersley DL, Lundblad JL. A new preparation of modified immune serum globulin (human) suitable for intravenous administration II. Functional characterization. *Vox Sang* 1981;40:383–394.
14. In: Garvey JS, Cremer NE, Sussdorf DH. eds. *Methods in immunology, third edition*. London: W.A. Benjamin Inc; 1977:267–270.
15. Petersen JGL, Dorrington KJ. An in vitro system for studying the kinetics of interchain disulfide bond formation in immunoglobulin G. *J Biol Chem* 1974;249:5633–5641.
16. Herscheid JDM, Hoekstra A, Vos CM. N-Succinyldesferrioxamine B: a potential radiopharmaceutical for assessing renal function. *Eur J Nucl Med* 1984;9:508–510.
17. Sakahara H, Endo K, Koizumi M, et al. Relationship between in vitro binding activity and in vivo tumor accumulation of radiolabeled monoclonal antibodies. *J Nucl Med* 1988;29:236–240.
18. Koizumi M, Endo K, Kunimatsu M, et al. Gallium-67-labeled antibodies for immunoscintigraphy and evaluation of tumor targeting of drug-antibody conjugate in mice. *Cancer Res* 1988;48:1189–1194.
19. Mather SJ, Ellison D. Reduction-mediated technetium-99m labeling of monoclonal antibodies. *J Nucl Med* 1990;31:692–687.
20. Grassetti DR, Murray JF, Jr. Determination of sulfhydryl groups with 2,2'- or 4,4'-dithiodipyridine. *Arch Biochem Biophys* 1967;119:41–49.
21. Imai S, Morimoto J, Tsubura T, et al. Genetic marker patterns and endogenous mammary tumor virus genes in inbred mouse strains in Japan. *Exp Anim* 1986;35:263–273.
22. Yokota T, Milenic DE, White M, Schlom J. Rapid tumor penetration of a single-chain Fv and comparisons with other immunoglobulin forms. *Cancer Res* 1992;52:3402–3408.
23. Anderson DC, Nichols E, Manger R, Woodle D, Barry M, Fritzberg AR. Tumor cell retention of antibody Fab fragment is enhanced by an attached HIV protein-derived peptide. *Biochem Biophys Res Commun* 1993;194: 876–884.